Zigzag and Eckhaus instabilities in a quintic-order nonvariational Ginzburg-Landau equation

R. B. Hoyle
Department of Applied Mathematics and Theoretical Physics, Silver Street, Cambridge CB3 9EW, United Kingdom
(Received 4 June 1998)

A nonvariational Ginzburg-Landau equation with quintic and space-dependent cubic terms is investigated. It is found that the equation permits both sub- and supercritical zigzag and Eckhaus instabilities and further that the zigzag instability may occur for patterns with wave number larger than critical ($q>0$), in contrast to the usual case. [S1063-651X(98)02712-3]

PACS number(s): 47.20.Ky

I. INTRODUCTION

Striped patterns, from convection rolls to sand ripples, are abundant in nature. The basic cellular pattern sets in above a critical value of the external stress at a favored wavelength selected by the system. Close to onset, the pattern is modulated on long space and time scales, as described by variations in its complex amplitude. In a two-dimensional isotropic environment, the amplitude is usually expected to evolve according to the Ginzburg-Landau equation

$$A_T=\mu A-|A|^2A+(\partial_X-\tfrac{1}{2}i\partial_{YY})^2A, \tag{1}$$

derived by Newell and Whitehead [1] and Segel [2]. However, in some cases the coefficient of the cubic term is small at onset, so the expansion can no longer be truncated at cubic order and must include higher-order terms, leading to the equation

$$A_T=\mu A+\alpha|A|^2A-|A|^4A+i\beta A^2(\partial_X+\tfrac{1}{2}i\partial_{YY})\overline{A}+i\gamma|A|^2(\partial_X-\tfrac{1}{2}i\partial_{YY})A+(\partial_X-\tfrac{1}{2}i\partial_{YY})^2A. \tag{2}$$

This equation is relevant to binary convection at small Lewis number [3,4]. In contrast to the usual equation (1), the amplitude equation (2) is nonvariational. The stability of roll solutions in the one-dimensional version of this equation ($\partial_Y=0$) was investigated by Eckhaus and Iooss [7].

The body of this paper investigates the stability to long-wavelength disturbances of stationary roll solutions of the nonvariational amplitude equation (2), determines the sub- or supercriticality of the bifurcations, and illustrates the behavior with numerical simulations.

II. PHASE INSTABILITIES

The leading-order amplitude equation for rolls $u(x,y,t)=A(X,Y,T)e^{ix}+\text{c.c.}$ in a homogeneous, isotropic two-dimensional environment in the case where the coefficient of the cubic term is small at onset is Eq. (2) above. The parameters μ, α, β, and γ are real constants. The equation is equivariant under x reflection $(X\to -X, A\to\overline{A})$ and y reflection $(Y\to -Y)$. Isotropy of the environment requires that the derivatives occur in combinations of $(\partial_X-\tfrac{1}{2}i\partial_{YY})A$ [5,6]. This last point is made clear by expressing rolls at an angle θ,

$$u=A_\theta e^{ix\sin\theta+iy\cos\theta}+\text{c.c.}, \tag{3}$$

in terms of the original roll solution giving

$$u=A_\theta e^{ix(\sin\theta-1)+iy\cos\theta}e^{ix}+\text{c.c.} \tag{4}$$

Since the environment is isotropic, neither A_θ nor the amplitude equation governing its evolution can depend on θ, so we must have a combination of derivatives that acts on $e^{ix(\sin\theta-1)+iy\cos\theta}$ to give zero. The combination $\partial_X-\tfrac{1}{2}i(\partial_{YY}+\partial_{XX})$ satisfies this requirement. However, the term $-\tfrac{1}{2}i\partial_{XX}$ is higher order than the other terms and so is omitted.

The amplitude equation was derived in the one-dimensional case by Eckhaus and Iooss [7]. It contrasts with the more usual form of the amplitude equation [1,2], where the coefficient of the cubic term is of unit order at onset. There is no Lyapunov functional for the present amplitude equation and the system is nonvariational. At $\mu=0$ the trivial solution $A=0$ undergoes a pattern-forming instability. Close to onset, the scalings are $\mu\sim O(\epsilon^2)$, $A\sim O(\epsilon^{1/2})$, $\partial/\partial X\sim O(\epsilon)$, $\partial/\partial Y\sim O(\epsilon^{1/2})$, $\alpha\sim O(\epsilon)$, β, and $\gamma\sim O(1)$, with $|\epsilon|\ll 1$.

The amplitude and wave number of stationary roll solutions $A=R_0e^{iqX}$, with R_0 and q real constants, are related by

$$O=\mu-q^2+\{\alpha+(\beta-\gamma)q\}R_0^2-R_0^4. \tag{5}$$

Making the perturbation $A=R_0e^{iqX}(1+a)$ with $|a|\ll 1$ gives

$$\begin{aligned}a_T={}&\alpha R_0^2(a+\overline{a})-2R_0^4(a+\overline{a})+2iq(\partial_X-\tfrac{1}{2}i\partial_{YY})a\\&+(\partial_X-\tfrac{1}{2}i\partial_{YY})^2a+(\beta-\gamma)qR_0^2(a+\overline{a})\\&+i\beta R_0^2(\partial_X+\tfrac{1}{2}i\partial_{YY})\overline{a}+i\gamma R_0^2(\partial_X-\tfrac{1}{2}i\partial_{YY})a.\end{aligned} \tag{6}$$

Considering long wavelength perturbations [$\partial_X,\partial_Y\sim O(\delta)$, $|\delta|\ll 1$], the amplitude perturbation $(a+\overline{a})$ evolves according to

$$(a+\overline{a})_T=2[\{\alpha+(\beta-\gamma)q\}R_0^2-2R_0^4](a+\overline{a})+O(\delta^2). \tag{7}$$

So the rolls are amplitude stable when

$$R_0^2>\tfrac{1}{2}\{\alpha+(\beta-\gamma)q\}, \tag{8}$$

as found by Eckhaus and Iooss [7].

A. Eckhaus instability

The phase behavior can be divided into Eckhaus and zigzag parts. If the perturbation a is dependent on X and T only there is an Eckhaus instability with the phase perturbation $(a-\overline{a})$ behaving according to the equation

$$(a-\overline{a})_T = c_1(a_{XX}-\overline{a}_{XX}) + c_2(a_{XXXX}-\overline{a}_{XXXX}) + O(\delta^6), \tag{9}$$

where

$$c_1 = 1 + \frac{[2q+(\beta+\gamma)R_0^2][2q-(\beta-\gamma)R_0^2]}{[2(\alpha+(\beta-\gamma)q)R_0^2-4R_0^4]}, \tag{10}$$

$$c_2 = \frac{(1-c_1)^2}{[2(\alpha+(\beta-\gamma)q)R_0^2-4R_0^4]}. \tag{11}$$

Setting $a-\overline{a}=\mathcal{A}e^{\sigma T+ikX}$, where $\mathcal{A}$ is a constant, shows that the Eckhaus instability occurs when

$$1 + \frac{[2q+(\beta+\gamma)R_0^2][2q-(\beta-\gamma)R_0^2]}{[2\{\alpha+(\beta-\gamma)q\}R_0^2-4R_0^4]} < 0, \tag{12}$$

as found by Eckhaus and Iooss [7].

Close to onset, the phase equation for the Eckhaus instability is given by

$$\phi_T = c_1\phi_{XX} + c_2\phi_{XXXX} + g(\phi_X^2)_X, \tag{13}$$

where $\phi=(a-\overline{a})\sim O(\delta)$, $c_1\sim O(\delta^2)$, c_2, and $g\sim O(1)$, $\partial_X\sim O(\delta)$, $\partial_T\sim O(\delta^4)$, and $|\delta|\ll 1$. The form of the nonlinear term is given by the scalings and the requirement that the equation should be equivariant under x reflection ($X\to -X$, $\phi\to-\phi$) and y reflection ($Y\to -Y, \phi\to\phi$).

The coefficient g of the nonlinear term can be found using Kuramoto's method [8]. Setting $\phi=\tilde{q}X+\tilde{\phi}$ in the phase equation (13) gives

$$\tilde{\phi}_T = (c_1+2g\tilde{q})\tilde{\phi}_{XX} + c_2\tilde{\phi}_{XXXX} + g(\tilde{\phi}_X^2)_X. \tag{14}$$

However, this is equivalent to letting $q\to q+\tilde{q}$, which would give the coefficient of $\tilde{\phi}_{XX}$ a value of $c_1+\tilde{q}(dc_1/dq)$ to leading order. It is then possible to identify $g=\frac{1}{2}(dc_1/dq)$.

Substituting the expression $\phi=\hat{a}(T)e^{ikX}+\hat{b}(T)e^{2ikX}$ + c.c. into the phase equation (13) leads to evolution equations for $\hat{a}(T)$ and $\hat{b}(T)$. A linear analysis of the $\hat{a}$ equation shows that the Eckhaus instability sets in for $c_1<k^2c_2\equiv c_{\rm cr}$ and then solving for $\hat{b}$ and substituting back into the $\hat{a}$ equation leads to an expression

$$|\hat{a}|^2 = \frac{(c_1-c_{\rm cr})(c_1-4c_{\rm cr})}{k^2g^2} \tag{15}$$

for the amplitude of stationary solutions. Thus, for $c_2>0$, $|\hat{a}|^2$ is positive for $c_1-c_{\rm cr}<0$, i.e., in the region of linear instability, so the bifurcation is supercritical, whereas for $c_2<0$, $|\hat{a}|^2$ is positive for $c_1-c_{\rm cr}>0$ and the instability is subcritical.

In the amplitude stable region, the coefficient c_2 is negative [Eq. (8)], so the instability is subcritical, whereas in the amplitude unstable region, the coefficient c_2 is positive and the instability is supercritical. In the usual real Ginzburg-Landau equation (1), rolls are amplitude stable whenever they exist and the Eckhaus instability is always subcritical, adjusting the wavelength of the pattern by creating phase slips in the pattern, where $|A|=0$ and the phase is undefined. Here the supercritical Eckhaus instability creates no defects as the pattern evolves towards a flat state ($q=0$) since the constant flat component of the solution grows faster than defects are formed by the Eckhaus instability (Fig. 1). The Eckhaus instability leads to flattening of the solution by increasing the pattern wavelength [Fig. 1(d)]. The numerical integration of Eq. (2) shown in Fig. 1 was performed using a pseudospectral code and periodic boundary conditions. The condition $\partial_Y=0$ was enforced by integrating the one-dimensional version of the equation.

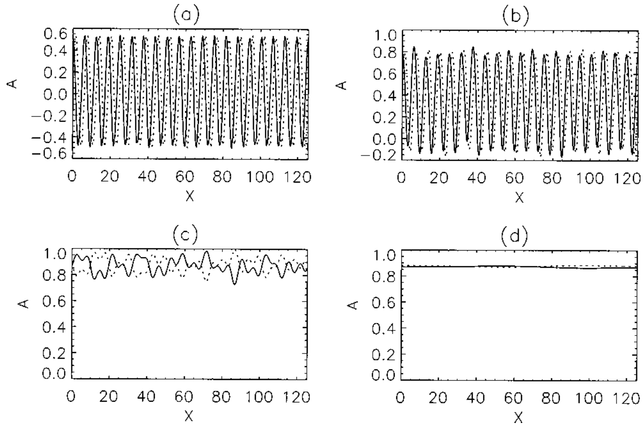

FIG. 1. Numerical simulation of the evolution of the supercritical Eckhaus instability. The initial roll state has $q=1.0$ and $R_0=0.5$ and the parameter values are $\mu=0.8125$ and $\alpha=\beta=\gamma=1.0$. The real (solid line) and imaginary (dotted line) parts of the amplitude A are plotted at times (a) $T=0.0$, (b) 2.0, (c) 4.0, and (d) 200.0.

B. Zigzag instability

In the zigzag instability where the perturbation varies only in the Y direction, the phase perturbation evolves according to the equation

$$(a-\overline{a})_T = \{q+\tfrac{1}{2}(\beta+\gamma)R_0^2\}(a_{YY}-\overline{a}_{YY}) - \tfrac{1}{4}(a_{YYYY}-\overline{a}_{YYYY}). \tag{16}$$

Instability sets in for $\{q+\frac{1}{2}(\beta+\gamma)R_0^2\}<0$. In contrast to the usual case, the zigzag instability can occur for $q>0$ if $(\beta+\gamma)<0$ and $q<-\frac{1}{2}(\beta+\gamma)R_0^2$. In this case the mechanism is expected to be different from the usual one where rolls at too long a wavelength ($q<0$) saturate into bends that decrease the wavelength.

The instability boundary $q=-\frac{1}{2}(\beta+\gamma)R_0^2$ is a parabola in (μ,q) space:

$$\mu = \frac{q}{(\beta+\gamma)^2}\{2\alpha(\beta+\gamma)+q[4+(3\beta-\gamma)(\beta+\gamma)]\}. \tag{17}$$

However, because for given μ and q there can be zero, one, or two corresponding values of R_0^2, only certain segments of the parabola act as stability boundaries (see Fig. 2). Depending on the parameter values, the zigzag curve can interact in many different ways with the neutral curve $\mu=q^2$ and the saddle-node curve $\mu=q^2-\frac{1}{4}\{\alpha+(\beta-\gamma)q\}^2$, which marks

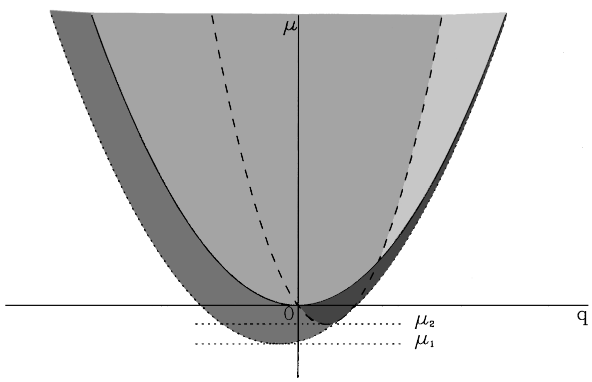

FIG. 2. Zigzag stability diagram for the case where there is strong rejection of patterns by the zigzag instability, $\{4-(\beta-\gamma)^2\}>0$, $\alpha>0$, and $\beta<0$. The parameter values are $\beta=-1.0$, $\gamma=-0.5$, and $\alpha=1.0$. The solid line is the neutral curve $\mu=q^2$, the dotted line is the saddle-node curve, and the dashed line is the zigzag instability boundary. In the lightest shaded region, there is one roll solution at each point (q,μ) and it is stable to the zigzag instability. In the second lightest region, there is one solution and it is zigzag unstable. In the second darkest region, there are two solutions at each point and they are both unstable to the zigzag instability. In the darkest shaded region there are two solutions and they are both zigzag stable. In the unshaded region there are no roll solutions. Note that for the range of μ between the two straight dotted lines, $\mu_1\equiv-\alpha^2/[4-(\beta-\gamma)^2]<\mu<-\alpha^2/[4+(3\beta-\gamma)(\beta+\gamma)]\equiv\mu_2$, all roll solutions are unstable to the zigzag instability. This is strong rejection of patterns.

the boundary between real and complex values of R_0^2. The latter two curves are drawn for various parameter values in Fig. 3 of Eckhaus and Iooss [7]. The zigzag curve is tangential to the saddle-node curve at $q=-\alpha(\beta+\gamma)/\{4+(\beta^2-\gamma^2)\}$. When $[4-(\beta-\gamma)^2]>0$, $\alpha>0$, and $\beta<0$, there is a range of values of μ, $-\alpha^2/[4-(\beta-\gamma)^2]<\mu<-\alpha^2/[4+(3\beta-\gamma)(\beta+\gamma)]$, for which roll solutions cannot be stable to the zigzag instability. Eckhaus and Iooss [7] found a similar phenomenon for the Eckhaus instability and termed it ''strong rejection of patterns''; here then is a ''strong rejection of patterns'' by the zigzag instability. The stability diagram is given in Fig. 2 for a case where there is strong rejection. Note also from the figure that where a roll solution with $q>0$ is unstable to the zigzag instability (in the second lightest shaded region, for example) it is possible that there is a stable roll solution with an even greater value of q at the same value of the forcing μ. Thus the zigzag bending of the rolls, which leads to a shorter wavelength, might in fact stabilize the pattern as it does in the $q<0$ case where the rolls are at a wavelength longer than critical.

The nonlinear phase equation close to onset is given by

$$\phi_T=c_3\phi_{YY}-\tfrac{1}{4}\phi_{YYYY}+h\phi_Y^2\phi_{YY}, \tag{18}$$

where $c_3=\{q+\frac{1}{2}(\beta+\gamma)R_0^2\}$. The equation is equivariant under x reflection $(X\rightarrow-X,\phi\rightarrow-\phi)$. and y reflection $(Y\rightarrow-Y,\phi\rightarrow\phi)$. The appropriate scalings are $\partial_T\sim O(\delta^4)$, $\partial_Y\sim O(\delta)$, $c_3\sim O(\delta^2)$, $\phi\sim O(1)$, and $h\sim O(1)$. Setting $\phi=pY+\tilde{\phi}$, substituting into the phase equation (18), and linearizing in $\tilde{\phi}$ gives

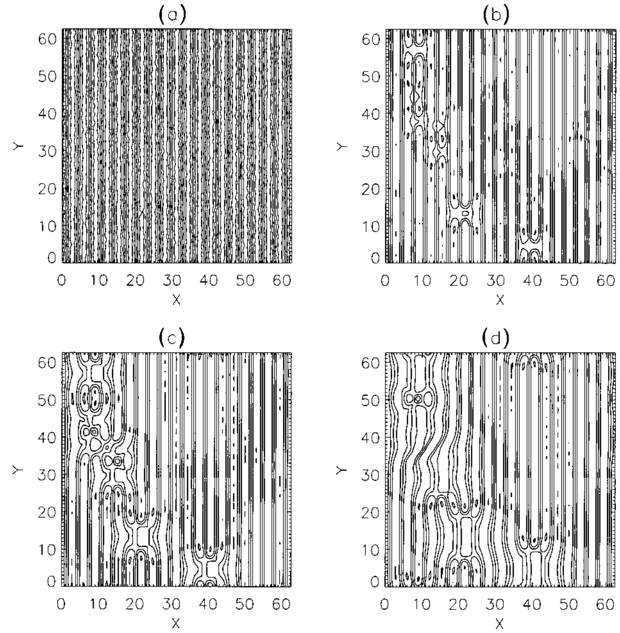

FIG. 3. Numerical simulation of the evolution of the zigzag instability in the subcritical case for rolls at larger than critical wavelength. The initial roll state has $q=-1.0$ and $R_0^2=1.0$ and the parameter values are $\mu=0.5$, $\alpha=-1.5$, $\beta=-0.75$, and $\gamma=2.25$. The real part of the amplitude A is given as a contour plot at times (a) $T=0.0$, (b) 6.0, (c) 12.0, and (d) 20.0.

$$\tilde{\phi}_T=(c_3+p^2h)\tilde{\phi}_{YY}-\tfrac{1}{4}\tilde{\phi}_{YYYY}. \tag{19}$$

However, this is equivalent to tilting the roll solution slightly to obtain a new roll solution with wave number $q+\frac{1}{2}p^2$, in which case the coefficient of $\tilde{\phi}_{YY}$ would be $c_3+\frac{1}{2}p^2(dc_3/dq)$ to leading order [9]. Hence it is possible to identify $h=\frac{1}{2}(dc_3/dq)$. If $h>0$, the nonlinear term is stabilizing, in that it makes a positive contribution to the effective diffusion coefficient, so the instability is supercritical, whereas if $h<0$ the nonlinear term is destabilizing and the instability is subcritical. The coefficient h can be found explicitly to be

$$h=\tfrac{1}{2}+\tfrac{1}{4}(\beta+\gamma)\,\frac{dR_0^2}{dq} \tag{20}$$

$$=\tfrac{1}{2}+\tfrac{1}{4}(\beta+\gamma)R_0^2\,\frac{[2q-(\beta-\gamma)R_0^2]}{[-\mu+q^2-R_0^4]}. \tag{21}$$

Figure 3 shows a numerical integration of Eq. (2) using a pseudospectral code with periodic boundary conditions in both directions. The initial state is a roll solution at negative wave number $(q<0)$ with random noise added and is stable to Eckhaus and amplitude modes, but unstable to the subcritical zigzag mode. The real part of the amplitude A is contoured at various times during the integration showing the evolution of the subcritical zigzag instability. Dislocations are formed in the pattern during the evolution from the initial unstable roll state. As can be seen from the left-hand side of the domain in Fig. 3(d), the pattern evolves towards rolls at a smaller value of $|q|$. Since q is negative, this cor-

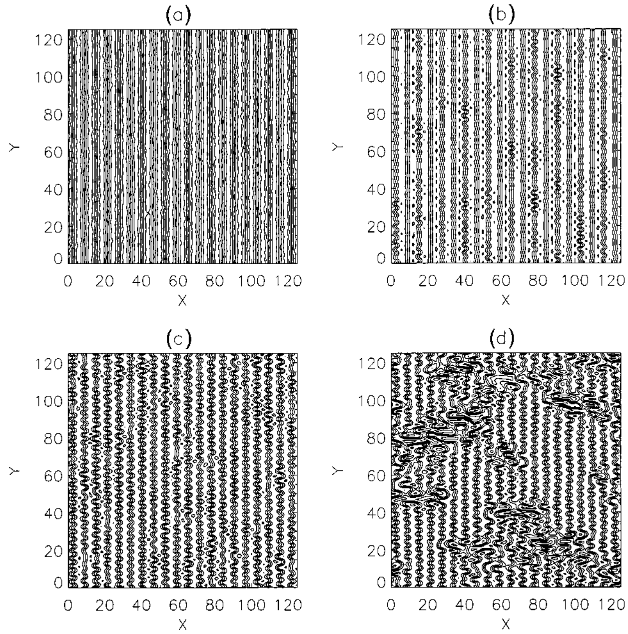

FIG. 4. Numerical simulation of the evolution of the zigzag instability in the supercritical case for rolls at smaller than critical wavelength. The initial roll state has $q=0.5$ and $R_0^2=1.0$ and the parameter values are $\mu=0.25$, $\alpha=1.0$, and $\beta=\gamma=-2.0$. The real part of the amplitude A is given as a contour plot at times (a) $T=0.0$, (b) 2.0, (c) 6.0, and (d) 60.0.

responds to a shorter wavelength overall. The formation of defects is a result of the subcriticality of the instability and contrasts with the phase diffusion that occurs in the more usual supercritical case.

Figure 4 shows the results of a numerical integration where the initial roll wave number is positive $(q>0)$ and the initial roll state is stable to Eckhaus and amplitude modes and unstable to the supercritical zigzag mode. Again the real part of the amplitude A is contoured at various times during the integration. The zigzag mode appears almost immediately at various points in the integration domain and diffuses along the roll axes until the entire domain is covered. The pattern finally develops patches of wiggles [Fig. 4(d)]. This contrasts with the usual case where the wave number is smaller than critical $(q<0)$ and the pattern saturates in an oblique mode at a larger wave number. With the parameter values of the numerical integration ($\alpha=1.0$, $\beta=\gamma=-2.0$, and $\mu=0.25$), there is one stable and one unstable roll solution in the range $0<q<(1+\sqrt{6})/5$. The initial pattern is an unstable roll solution in this range, but there do exist stable roll patterns with higher values of q. It is possible then that the patches of wiggles are stabilizing.

III. CONCLUSION

The phase instabilities of the nonvariational Ginzburg-Landau equation with quintic and space-dependent cubic terms (2) show interesting features. The Eckhaus instability is subcritical where roll solutions are amplitude stable and supercritical where roll solutions are amplitude unstable. The supercritical Eckhaus instability is unusual and arises because the amplitude instability causes a nonzero flat component of the solution to grow sufficiently fast that the Eckhaus mode evolves without causing phase slips.

The zigzag instability can occur not only for rolls with a longer than critical wavelength $(q<0)$ but also for rolls with a wavelength shorter than critical $(q>0)$. This seems counterintuitive since the zigzag bending mode acts to decrease the wavelength. However, in this system it can happen that rolls at even shorter wavelength (higher q) are stable. Further, the zigzag instability can be subcritical, creating defects in the pattern, in contrast to the usual supercritical case.

[1] A. C. Newell and J. A. Whitehead, J. Fluid Mech. **38**, 279 (1969).
[2] L. A. Segel, J. Fluid Mech. **38**, 203 (1969).
[3] W. Schöpf and W. Zimmermann, Europhys. Lett. **8**, 41 (1989).
[4] W. Schöpf and W. Zimmermann, Phys. Rev. E **47**, 1739 (1993).
[5] G. H. Gunaratne, Phys. Rev. Lett. **71**, 1367 (1993).
[6] G. H. Gunaratne, Q. Ouyang, and H. L. Swinney, Phys. Rev. E **50**, 2802 (1994).
[7] W. Eckhaus and G. Iooss, Physica D **39**, 124 (1989).
[8] Y. Kuramoto, Prog. Theor. Phys. **71**, 1182 (1984).
[9] S. Fauve, Woods Hole Oceanographic Institution Technical Report No. WHOI-92-16, p. 74, 1991 (unpublished).